

Measurement of the infrared transmission through a single doped GaAs quantum well in an external magnetic field: Evidence for polaron effects

C. Faugeras,¹ M. Orlita,^{1,2} S. Deuchlander,¹ G. Martinez,¹ P. Y. Yu,³ A. Riedel,⁴ R. Hey,⁴ and K. J. Friedland⁴

¹Grenoble High Magnetic Field Laboratory, CNRS, BP 166, 38042 Grenoble Cedex 9, France

²Institute of Physics, Charles University, Ke Karlovu 5, CZ-121 16 Praha 2, Czech Republic

³Department of Physics, University of California at Berkeley, Berkeley, California 94720, USA

⁴Paul Drude Institute, Hausvogteiplatz 5-7, D-10117 Berlin, Germany

(Received 15 July 2009; published 20 August 2009)

Precise absolute far-infrared magnetotransmission experiments have been performed in magnetic fields up to 33 T on a series of single GaAs quantum wells doped at different levels. The transmission spectra have been simulated with a multilayer dielectric model. The imaginary part of the optical response function which reveals singular features related to the electron-phonon interactions has been extracted. In addition to the expected polaronic effects due to the longitudinal-optical phonon of GaAs, a kind of carrier-concentration-dependent interaction with interface phonons is observed. A simple physical model is used to try to quantify these interactions and explore their origin.

DOI: [10.1103/PhysRevB.80.073303](https://doi.org/10.1103/PhysRevB.80.073303)

PACS number(s): 78.67.De, 71.38.-k, 78.30.Fs, 78.66.Fd

Polaronic effects, due the Fröhlich interaction between electrons and the longitudinal-optical (LO) phonon of a polar semiconductor, have been the object of many reports.¹⁻³ In quasi-two-dimensional (Q2D) GaAs-based structures, there is evidence of free polaronic effects (PE) but few experiments^{4,5} have focused on cyclotron resonance (CR) in the region above the Reststrahlen band energy (RBE) of GaAs (this requires for GaAs a magnetic field strength beyond 23 T). Theoretically PE were first studied by Lee and Pines⁶ and later by Feynman.⁷ It was realized that this kind of interaction could not be properly handled by perturbation theory and requires a global treatment. Such an approach was proposed by Feynman *et al.*,⁸ and referred to as the Feynman–Hellwarth–Iddings–Platzman (FHIP) model. It has been invoked to explain the polaronic mass and later extended by Peeters and Devreese⁹ to extract the conductivity of the Q2D electron gas in the presence of PE. In the latter case, its major effects are expected to be observed in the imaginary part of the response function at energies larger than the RBE. This prediction has motivated the present study.

Far-infrared magneto-optical experiments have been performed at magnetic field strengths up to 33 T and at a fixed temperature of 1.8 K, on a series of single modulation-doped quantum wells (QW) of width $L=13$ nm with different doping levels N_s ranging from 2 to 7.7×10^{11} cm⁻² and mobility exceeding 10^6 cm²/(V s). The structure of these samples is similar to those reported earlier:⁵ a single GaAs QW is sandwiched between two GaAs-AlAs superlattices δ -doped symmetrically with Si- n -type dopant on both sides of the QW. In the present case however the epilayer is not lifted-off from the GaAs substrate. As a result the samples are optically opaque in the RBE range. For each fixed value of the magnetic field B , an *absolute* magneto infrared transmission spectrum $[TA(B, \omega)]$ is measured by using a rotating sample holder containing a hole to obtain a reference spectrum under the same conditions as for the sample. The Faraday configuration is used with the \mathbf{k} vector of the incoming light parallel to \mathbf{B} and also to the growth axis (100) of the sample. These

spectra $TA(B, \omega)$ are in turn divided by $TA(0, \omega)$ to obtain the *relative* transmission spectra $TR(B, \omega)$ which will be displayed in the present paper. The analysis of these spectra is based on a multilayer dielectric model.¹⁰ This is essential because, in the frequency range of interest, the spectra can be distorted by dielectric interference effects even in the absence of electron-phonon interactions.

The $TR(B, \omega)$ spectra of two characteristic samples, sample MA-2226 ($N_s=3 \times 10^{11}$ cm⁻²) and sample MA-1490 ($N_s=6.3 \times 10^{11}$ cm⁻²), are displayed in Figs. 1(a) and 1(d) respectively. For sample MA-2226, the CR absorption almost vanishes just above the RBE for $B \approx 24$ T. But as B is increased beyond 24 T it starts to increase and also its line shape changes with field. A “singularity” appears to occur when the CR energy approaches 45 meV [the transverse-optical (TO)-phonon energy of AlAs as measured in the $TA(0)$ spectrum] at $B \approx 27$ T. Its linewidth peaks when its energy is around 48 meV ($B \approx 29$ T) before recovering its original line shape below the RBE at even higher fields. In contrast, for sample MA-1490, the CR transition is clearly seen when it first emerges above the RBE, its line shape has broadened already when its energy is around 38 meV ($B \approx 24.5$ T), it shows some singular behavior at 45 meV ($B \approx 28$ T) while its linewidth appears to reach a maximum at the same time. Finally it recovers the original low-fields line shape for $B > 32$ T.

To simulate these complex spectra, we start with the dielectric function $\bar{\epsilon}$ of the doped QW in addition to the appropriate dielectric functions of undoped barrier layers.¹⁰ For the doped QW, the diagonal part ϵ_{xx} is written as

$$\epsilon_{xx} = \epsilon_L - \frac{\omega_p^2}{\omega\{\omega - [\omega_{NP} - \text{Re}(\Sigma)] + i[\eta + \text{Im}(\Sigma)]\}} \quad (1)$$

in which the x axis is assumed to lie in the plane of the QW, ϵ_L is the contribution of the GaAs lattice, ω_{NP} is the contribution to the CR frequency of the nonparabolicity (NP) effects,¹¹ η is the field-independent contribution of the background defects to the linewidth while $\Sigma(\omega)$ represents the

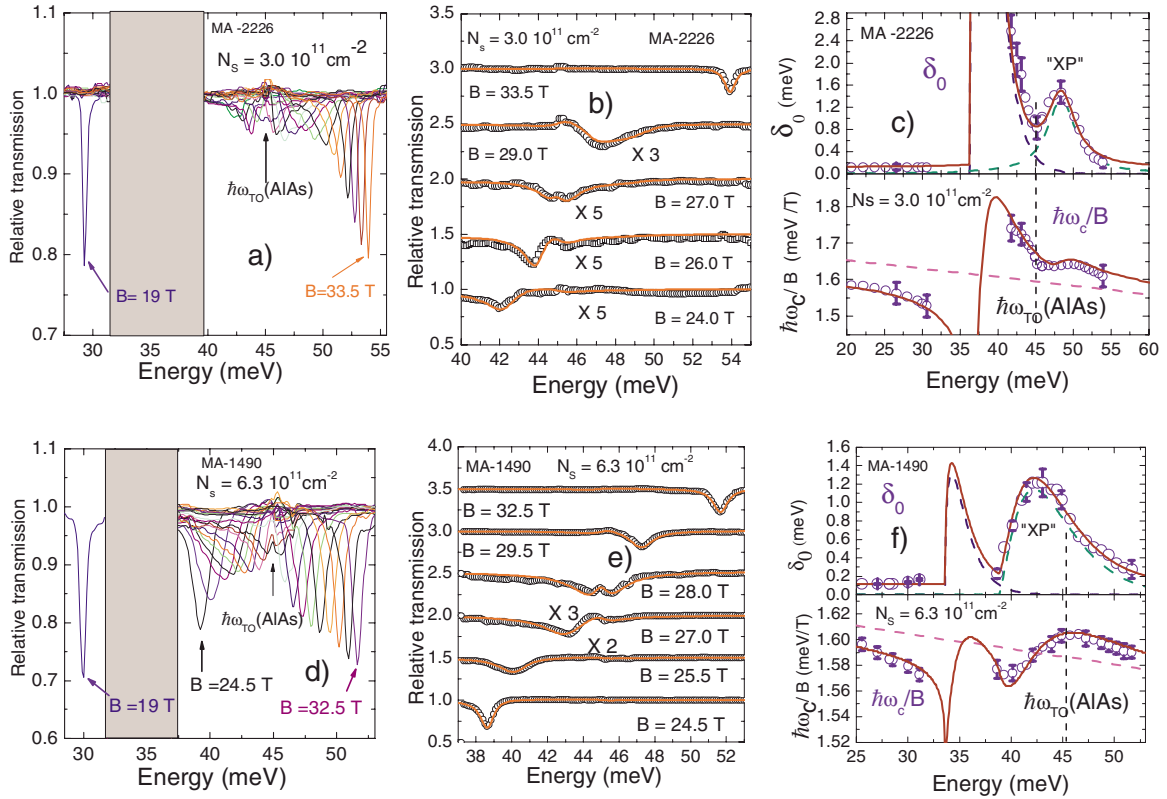


FIG. 1. (Color online) [(a) and (d)]: Relative transmission spectra of samples MA-2226 and MA-1490, respectively, for different magnetic fields. [(b) and (e)]: Simulation of some experimental spectra (open dots) with the multidiagonal model (continuous curve): each curve is shifted by 0.5 with a scale enlarged as noted. [(c) and (f)]: Fitted parameters $\hbar\omega_c/B$ and δ_0 as extracted from Eq. (1) (open dots) for both samples; the dashed lines in the upper panels (δ_0) are the resulting decomposition of the polaronic and XP interactions adopted to fit $\text{Im}(\Sigma)$; the total contributions of the interaction [continuous curves in (c) and (f)] are used to simulate the spectra in (b) and (e), respectively; the oblique dashed lines in the lower panels of (c) and (f) mimic the nonparabolicity contribution with the corresponding energy scale (see text).

self-energy correction due to interactions between the electron gas and elementary excitations to be discussed further. The effective mass m^* entering the plasma frequency ω_p is calculated with the same NP model. We note that the line shape and intensity of the CR transitions at low and high fields are practically the same. Hence we can assume that there is no loss of carrier density during the magnetic field runs. In the fitting process, we *first* neglect the frequency dependence of Σ and are left with two independent parameters $\omega_c = \omega_{\text{NP}} - \text{Re}(\Sigma)$ and $\delta_0 = \eta + \text{Im}(\Sigma)$ for each magnetic field. The resultant parameters ($\hbar\omega_c/B$ and δ_0) are displayed in Figs. 1(c) and 1(f) (open dots) as a function of the energy $\hbar\omega_c(B)$ (in these figures some typical error bars reflect the estimated uncertainties of the fitting procedure). From these plots we notice that below the RBE, δ_0 is constant and weak being determined mainly by η . Above the RBE there are sudden and large increases in δ_0 for both samples. However their behaviors are quite different. For sample MA-2226, there are two distinct contributions to δ_0 : one lower field component starts very large but decreases strongly with field and a second component which starts from almost zero but goes through a maximum at B corresponding to about 48 meV. For the time being we will label the interaction which contributes to this peak in δ_0 as XP. For sample MA-1490, only the XP contribution to δ_0 is observed. In this case the peak occurs at B corresponding to 42 meV.

Thus our results suggest that there are two kinds of excitations interacting with the Q2D electron gas at high fields: one which is observed in the lower doped samples and another one labeled as XP which is observed in both samples. Very similar results have been obtained with another sample MA-2227 doped at the level $N_s = 2 \times 10^{11} \text{ cm}^{-2}$. In this sample the first interaction is a little bit stronger than for sample MA-2226 while the XP peak is quite similar. We assign the first interaction to polaronic effects since it appears to peak at fields when the CR frequency will resonate with the GaAs LO phonon frequency (slab mode). This assignment is consistent with the observation that this interaction is very sensitive to the carrier concentration. In sample MA-1490 this interaction seems to have disappeared from δ_0 . We note that in a previous report,⁵ on lift-off samples more highly doped in the range of $N_s = 7-9 \times 10^{11} \text{ cm}^{-2}$, only some weak interaction around the TO of GaAs was observed. This result was later on analyzed by Klimin *et al.*¹² as PE with the LO phonon screened by electrons to the point that its value becomes close to the TO phonon frequency. The same analysis can be applied to the sample MA-1490 and other higher doped samples.

To mimic PE we restrict ourselves to one polaron first and, using the FHIP model, write down $\text{Im}[\Sigma(\omega)]$ as⁹

$$\text{Im}[\Sigma(\omega)] = \omega_{\text{LO}} \frac{\omega_0}{\omega} \alpha F |A_0(\omega)|^{1/2} e^{-R|A_0(\omega)|} \Theta(A_0(\omega)), \quad (2)$$

where $A_0(\omega) = \omega/\omega_0 - 1$, $\Theta(x) = 1$ for $x > 1$ or zero otherwise. In the absence of screening $\omega_0 = \omega_{\text{LO}}$. If ω_0 is known, Eq. (2) depends on two parameters αF and R . The FHIP model, developed in a one-electron picture, assumes that electron-phonon interaction is harmonic instead of Coulombic as in the case of the Fröhlich interaction. The model depends on two parameters: v and w in reduced units of ω_{LO} . One of them (w) is close to 1 while $v^2 - w^2$ represents the force constant of the harmonic interaction (equivalent to the Fröhlich constant α). In this case $R = (v^2/w^2 - 1)/v$ whereas αF is a global quantity which depends on v and w but should also imply corrections for the dimensionality of the problem and for screening effects. The present approach can be regarded as a test of the FHIP model when applied to Q2D electrons under high magnetic fields.

Using this simplified model, one can fit the data on δ_0 for the polaronic contribution. For sample MA-2226 we have to add contribution for the XP interaction [Fig. 1(c), upper panel]. If we assume that the XP interaction satisfies the linear-response function theory, then $\text{Im}[\Sigma(\omega)]$ and $\text{Re}[\Sigma(\omega)]$ are related by the Kramers-Krönig (KK) relations. The resultant constraint on the fitting process is that the KK transformation of $\delta_0(\omega)$ should reproduce the variation in $\hbar\omega_c(\omega)/B$. One has also to fit the NP effects, $\hbar\omega_{\text{NP}}(B)/B$ versus $\hbar\omega_{\text{NP}}(B)$ with standard models¹¹ [dashed oblique lines in Fig. 1(c)] but this corresponds simply to a global shift of the curves. The fitted functions $\hbar\omega_c(\omega)/B$ and $\delta_0(\omega)$ are then inserted in the multilayer dielectric model from which one can compute, for each value of B , the TR spectrum and compare it to the corresponding experimental spectrum [Fig. 1(b)]. The agreement is quite satisfactory as one can see from that figure. However, it is clear that the fitting of PE is not unique for these reasons: (i) we have assumed for sample MA-2226 that $\omega_0 = \omega_{\text{LO}}$ neglecting, therefore, screening effects, (ii) we have treated the problem with one polaron instead of several polarons. Even if this effect does not influence $\text{Im}[\Sigma(\omega)]$, the KK transformation depends on *all* contributions to $\text{Im}[\Sigma(\omega)]$ including those at higher energies than we can reach experimentally. The same procedure has been applied to simulate the data on sample MA-1490, but here we have assumed a weakened PE starting near the TO phonon energy of GaAs in order to reproduce the nonlinearity of $\hbar\omega_c(\omega)/B$ below the RBE [lower panel of Fig. 1(f)]. The choice of the corresponding fitting parameters in Eq. (2) is now completely arbitrary. We can also reproduce quite well the experimental transmission spectra as shown in Fig. 1(e).

Although we do not know the value of the prefactor αF in Eq. (2), it is instructive to compare the parameter R entering this equation. One finds $R \approx 25$ and 18 for samples MA-2227 and MA-2226, respectively. These values could, of course, be lowered if one assumes some screening of the LO phonon in Eq. (2) and if we include higher polarons in the analysis but they remain, at least, an order of magnitude higher than that proposed ($R=0.04$) for unscreened PE.¹³ These values imply that the v and w parameters in the FHIP model have to

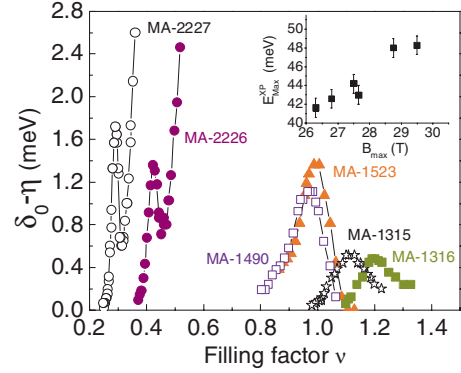


FIG. 2. (Color online) Variation in $\text{Im}(\Sigma)$ with the filling factor ν for different samples: MA-2227 with open dots ($N_s = 2 \times 10^{11} \text{ cm}^{-2}$), MA-2226 with full dots ($N_s = 3 \times 10^{11} \text{ cm}^{-2}$), MA-1490 with open squares ($N_s = 6.3 \times 10^{11} \text{ cm}^{-2}$), MA-1523 with full triangles ($N_s = 6.6 \times 10^{11} \text{ cm}^{-2}$), MA-1315 with open stars ($N_s = 7.1 \times 10^{11} \text{ cm}^{-2}$), and MA-1316 with full squares ($N_s = 7.7 \times 10^{11} \text{ cm}^{-2}$). Inset: Variation in the characteristic energies $E_{\text{max}}^{\text{XP}}$ of the maximum of the XP interaction with the corresponding magnetic field B_{max} (see text). The corresponding error bars take into account the nonsymmetric shape of the interaction.

be smaller than 1 even for the samples MA-2226 and MA-2227. This raises the question of the physical interpretation of these parameters: knowing that ω_{LO} cannot be smaller than ω_{TO} , it seems that a more physical approach should be to relate in some way these parameters to the TO-LO splitting rather than to a single frequency such as ω_{LO} .

We focus next on the discussion on the possible origins of the XP interaction. The variation in $\text{Im}(\Sigma) = \delta_0 - \eta$ is plotted in Fig. 2 for six different samples as a function of the filling factor $\nu = N_s \Phi_0 / B$, where Φ_0 is the flux quantum. The XP interaction which is *only* observed for energies larger than the RBE, clearly decreases for the higher doped samples (MA-1315 and MA-1316) and indeed disappears completely when $N_s \geq 9 \times 10^{11} \text{ cm}^{-2}$. This result indicates that the XP interaction is strongly screened by free electrons. The energy $E_{\text{max}}^{\text{XP}}$ corresponding to the maximum of this interaction decreases while the corresponding value $\nu_{\text{max}}^{\text{XP}}$, the value of ν where this maximum occurs, increases or $E_{\text{max}}^{\text{XP}}$ increases with the corresponding value of B_{max} (insert of Fig. 2). This interaction is clearly dissipative and in these samples of very high mobility, is unlikely to be caused by impurities. We are then left with intrinsic mechanisms such as electron-phonon interaction as a plausible explanation knowing that in these samples the intersubband energy is on the order of 65 meV (Refs. 5 and 10) and cannot play a role. In a GaAs QW, sandwiched between AIAs layers, several kinds of optical phonons are present. The most well known ones are the confined phonons (slab modes) mainly associated with mechanical motion of atoms. The frequency of these modes lies inside the RBE. The other phonons of dielectric origin (which could be hence screened by free carriers) are the interface phonons. Because of the reflection symmetry of the GaAs QW with respect to its center, these modes are divided into either symmetric or antisymmetric modes.¹⁴ The symmetric modes which are infrared active have been invoked in Ref. 4 to explain the “splitting” of the CR transition observed near

$\hbar\omega_{\text{TO}}(\text{AlAs})$ (45 meV). Such splitting is observed also in *all* our samples including the very heavily doped samples (up to $N_s=1.9\times 10^{12}\text{ cm}^{-2}$). As seen in Figs. 1(b) and 1(e), it can be perfectly reproduced by our simulation with the multilayer dielectric model as a result of pure interference effects in the transmission spectra. We also note that the wave function of these symmetric interface modes does not vanish at the center of the QW (unlike the antisymmetric modes) and therefore have significant overlap with the wave function of the Q2D gas. Thus the idea of possible interaction between the interface modes and the Q2D electron gas deserves more detailed analysis. The solutions for these modes between a GaAs layer sandwiched between two AlAs layers are given by¹⁴

$$\varepsilon_{\text{AlAs}} = -\varepsilon_{\text{GaAs}} \times \tanh(q_{\parallel}L/2), \quad (3)$$

where q_{\parallel} is the wave vector of the interface electromagnetic wave traveling parallel to the plane of the Q2D gas. In the absence of magnetic field, the two solutions of Eq. (3) lie in the Reststrahlen bands of GaAs and AlAs. But, when the magnetic field effect is included in $\varepsilon_{\text{GaAs}}$, through Eq. (1) for instance, the results are different: (i) depending on the parameters the number of solutions of Eq. (3) can be larger than 2, (ii) some of the solutions are now strongly dependent on the magnetic field and can extend to energies higher than $\hbar\omega_{\text{TO}}(\text{AlAs})$ as observed here. When increasing N_s , one would expect that an interaction with the Q2D electron gas will result in a downshift (or renormalization) of the interface mode energy in a way similar to what is observed for the polaronic effects in Figs. 1(c) and 1(f). This effect has never been investigated to our knowledge but certainly deserves further studies. In particular, it is desirable to under-

stand the mechanism of electron-phonon interaction which makes this interaction resonant for a specific energy $E_{\text{max}}^{\text{XP}}$.

At present we prefer the explanation of the XP interaction in terms of interface modes though we cannot exclude more speculative interpretations, such as, strong nonlinear effects of the polaronic interaction.

It is clear that in order to get a deeper and more definitive understanding into all the interactions between the Q2D electrons and other elementary excitations such as phonons, one should obtain experimental results on lift-off samples which can provide more unambiguous values of the threshold energies related to the simple polaronic effect.

In conclusion, we have performed infrared magneto-optical transmission measurements of a Q2D electron gas in a single modulation-doped GaAs QW with different densities, for magnetic fields high enough to scan the cyclotron resonance frequency beyond the Reststrahlen band of GaAs. From the experimental spectra, we have extracted the imaginary part of the response function which reveals several singularities whose number and strength depend on the carrier density. These singularities have been attributed to electron-phonon interactions. One of these interactions involving the LO phonon of GaAs has been treated with a simplified version of the FHIP polaronic model. But to explain all our results quantitatively, it is necessary to invoke a more elaborate theory which includes effects of screening and possible interaction with interface modes.

The GHMFL is ‘‘Laboratoire conventionn e   l’UJF de Grenoble.’’ This work has been supported in part by the European Commission through Grant No. RITA-CT-2003-505474. G.M. and P.Y.Y acknowledge support of a grant from the France-Berkeley fund.

¹J. T. Devreese, J. Phys.: Condens. Matter **19**, 255201 (2007), and references herein.

²P. Gaal, W. Kuehn, K. Reimann, M. Woerner, T. Elsaesser, and R. Rey, Nature (London) **450**, 1210 (2007).

³Yu. Chen, N. Regnault, R. Ferreira, B.-F. Zhu, and G. Bastard, Phys. Rev. B **79**, 235314 (2009).

⁴Y. J. Wang, H. A. Nickel, B. D. McCombe, F. M. Peeters, J. M. Shi, G. Q. Hai, X.-G. Wu, T. J. Eustis, and W. Schaff, Phys. Rev. Lett. **79**, 3226 (1997).

⁵C. Faugeras, G. Martinez, A. Riedel, R. Hey, K. J. Friedland, and Yu. Bychkov, Phys. Rev. Lett. **92**, 107403 (2004).

⁶T. D. Lee and D. Pines, Phys. Rev. **92**, 883 (1953).

⁷R. P. Feynman, Phys. Rev. **97**, 660 (1955).

⁸R. P. Feynman, R. W. Hellwarth, C. K. Iddings, and P. M. Platzman, Phys. Rev. **127**, 1004 (1962).

⁹F. M. Peeters and J. T. Devreese, Phys. Rev. B **28**, 6051 (1983).

¹⁰Yu. Bychkov, C. Faugeras, and G. Martinez, Phys. Rev. B **70**, 085306 (2004).

¹¹C. Hermann and C. Weisbuch, Phys. Rev. B **15**, 823 (1977).

¹²S. N. Klimin, V. M. Fomin, and J. T. Devreese, Phys. Rev. B **77**, 205311 (2008).

¹³F. M. Peeters and J. T. Devreese, Phys. Rev. B **25**, 7281 (1982).

¹⁴N. Mori and T. Ando, Phys. Rev. B **40**, 6175 (1989).